

# Numerical Investigation of the Bias Voltages Effects on the Performance of Plasmonic HEMTs

**Farzaneh Daneshmandian**

Dept. Electrical Engineering,  
Amirkabir University of  
Technology  
Microwave/mm-Wave &  
Wireless Communication  
Research Lab  
Tehran, Iran  
f.daneshmandian@aut.ac.ir

**Abdolali Abdipour\***

Dept. Electrical Engineering,  
Amirkabir University of  
Technology  
Microwave/mm-Wave &  
Wireless Communication  
Research Lab  
Tehran, Iran  
abdipour@aut.ac.ir

**Amir Nader Askarpour**

Dept. Electrical Engineering,  
Amirkabir University of  
Technology  
Microwave/mm-Wave &  
Wireless Communication  
Research Lab  
Tehran, Iran  
askarpour@aut.ac.ir

Received: 18 December 2018 - Accepted: 30 December 2018

**Abstract**— The two dimensional (2D) plasmon propagation in the channel of a high electron mobility transistor (HEMT) is numerically analyzed using the full wave method. By applying different bias voltages to the drain and the gate terminals, the properties of the 2D plasmons propagation along the channel are investigated. In this analysis, the Maxwell's equations are solved in conjunction with the hydrodynamic transport equations, using the finite difference time domain (FDTD) technique. The obtained results show that the wavelengths and the propagation constants of the 2D plasmons are considerably affected by varying the bias voltages. Then, by considering these effects, the tunability of a grating gate HEMT detector over terahertz (THz) frequencies is investigated, using the proposed full wave model. Our studies demonstrate that it is possible to control the characteristics of the 2D plasmon propagation along the channel by changing the bias voltages to produce various types of reconfigurable structures used for THz applications.

**Keywords**-component; 2DEG channel; 2D plasmon; full wave model; hydrodynamic equations; HEMT structure; resonant detector

## I. INTRODUCTION

Applications of the terahertz (THz) technology in imaging, radar, sensing, and telecommunications, have instigated many research efforts in this field [1]-[3]. Many Plasmonic devices such as compact THz switches, detectors and sources are implemented based on the two dimensional electron gas (2DEG) layers of hetero-structures [4],[5]. By confining the electromagnetic waves along the 2DEG channels of the high electron mobility transistors (HEMTs), the 2D

plasmon can propagate efficiently at THz frequencies. Such structures are suitable for design and implementation of many nano-scale plasmonic devices [6]-[8].

An accurate analysis and modeling of these plasmonic HEMT devices are important in THz frequencies. Already, some studies are reported to model these structures analytically and numerically. In [9], the properties of the 2D plasmon propagation in the 2DEG channels of the ungated and the gated biased hetero-structures are characterized analytically.

\* Corresponding Author

Moreover, several numerical investigations based on the hydrodynamic full wave model are accomplished to analyze the wave propagation along the HEMT channel [10],[11]. The hydrodynamic full wave modeling method is achieved by solving the coupled set of Maxwell's and electronic transport equations and describes completely the electron-wave interactions along the 2DEG channel of HEMT structures [12],[13].

In this paper, a numerical analysis method based on the hydrodynamic full wave model is used to characterize the 2D plasmon propagation along the 2DEG layer under different bias voltages. Indeed, by applying various bias voltages to the drain and gate contacts of the ungated/gated HEMT, the characteristics of the plasma waves are studied numerically. Also, as an example of the bias voltages effects, the tunability of a grating gate HEMT is analyzed. To solve the coupled set of highly nonlinear hydrodynamic model equations numerically, the finite difference time domain (FDTD) method is used. To reduce the numerical calculations and consequently reduction of the total simulation time, a non-uniform mesh grid is employed. It is demonstrated that the plasmon properties can be controlled significantly by varying the bias voltages. This feature makes it possible to design various plasmonic HEMT structure, especially tunable THz detectors.

The proposed full wave hydrodynamic model equations are described in section II. Moreover, the analytical dispersion relations for the propagation of 2D plasmon are presented. In order to validate the proposed modeling approach, the numerical full wave results are compared with the analytical ones. Then by applying various voltages to the gate and the drain terminals, the properties of the plasmon propagation are studied, using the proposed full wave model in section III. In section IV, the analysis of a metallic grating HEMT as a tunable detector is investigated and its transmission spectra are extracted for various gate bias voltages.

## II. FULL WAVE MODEL

### A. Model Equations

To analyze the behavior of the wave propagation in the channel of plasmonic HEMTs in THz frequencies, the full wave hydrodynamic model that is the solution of the Maxwell's equations and the moments of the Boltzmann transport equation (BTE) is used. In the linear regime of the device operation it is only enough to consider the first two moments of the BTE, i.e. the particle conservation and the momentum conservation equations [10]. These two transport equations for a HEMT 2DEG layer placed along the  $x$ -axis are [14],[15]

$$\frac{\partial(nm^*v_x)}{\partial t} + qnE_x + \nabla \cdot (nm^*v_x\vec{v}) + \frac{\partial(nk_B T)}{\partial x} = -\frac{nm^*v_x}{\tau_m} \quad (1)$$

$$\frac{\partial n}{\partial t} + \nabla \cdot (n\vec{v}) = 0 \quad (2)$$

where  $E_x$  and  $k_B$  are the electric field and the Boltzmann constant along the channel. Moreover,  $\vec{v}$ ,

$n$ ,  $q$ ,  $T$ ,  $\tau_m$ , and  $m^*$  are the velocity, volume density, unit charge, temperature, momentum relaxation time, and effective mass of electron, respectively. The electromagnetic wave propagation in the cross section of the HEMT structure can be described by using the Maxwell's equations as

$$\nabla \times \vec{H} = \frac{\partial(\epsilon\vec{E})}{\partial t} + \vec{J}_v \quad (3)$$

$$\nabla \times \vec{E} = -\frac{\partial(\mu\vec{H})}{\partial t} \quad (4)$$

where  $\mu$  and  $\epsilon$  are the magnetic permeability and the electric permittivity of the semiconductor, respectively, and also  $\vec{J}_v$  is the electron current density in the channel of the HEMT. The coupling between the electronic transport and the electromagnetic solvers are through the current density as

$$\vec{J}_v = -qn\vec{v} \quad (5)$$

By solving the electronic transport and the Poisson equations simultaneously, the initial state of the analysis can be achieved. To reach the numerical solution, the nonlinear set of questions (1) - (5) must be solved self-consistently. The FDTD method is employed as a powerful numerical technique to solve these highly nonlinear coupled differential equations. First, the transport equations are solved using 1D-FDTD to attain the current density  $\vec{J}_v$ , then the obtained current density is fed to the Maxwell's equations to update the electric and magnetic fields in the cross section of the device, using 2D-FDTD. Afterwards, the new values of fields are used to update the transport model equations in the next time step. This process is continued to get the steady state solution.

### B. Validation the Model

To validate our modeling approach, the proposed full wave model is used to study the 2D plasmon characteristics in an ungated and a gated 2DEG layers, and the results are compared with those obtained analytically. The analytical dispersion relation for a gated 2DEG layer with the electron concentration  $n_0$  is obtained as [11]

$$k = \frac{\omega^2 m^* \epsilon}{n_0 q^2} (1 + \coth(kd_{barr})) \quad (6)$$

where  $k = 2\pi/\lambda$  and  $d_{barr}$  are the propagation constant and the distance between the top gate and the channel, respectively. Also, for an ungated 2DEG layer the dispersion relation is [11]

$$k = \frac{1}{2a^2} \sqrt{\omega^4 + \frac{4a^2 \omega^2 \epsilon_r}{c^2}} \quad (7)$$

where  $a = \frac{n_0 q^2}{4\epsilon m^*}$ ,  $c = 3 \times 10^8 \text{ m/s}$ , and  $\epsilon$  is the electric permittivity of the substrate surrounding the 2DEG layer.

The cross section of the InGaAs gated HEMT structure assumed for our analysis is demonstrated in Fig. 1. The drain and the source ohmic terminals are approximated to be Perfect Electric Conductors (PECs). This assumption is valid in most of the practical semiconductor devices [16]. The substrate is InGaAs with dielectric constant  $\epsilon_r = 13.9$ , thickness  $h = 3.5 \mu\text{m}$ , and  $d_{\text{barr}} = 30 \text{ nm}$ . The 2DEG channel length is  $L_c = 4 \mu\text{m}$ , which is large enough compared to the 2D plasmon wavelength in the frequency range of our analysis. Furthermore, the electron concentration  $n_0 = 1.5 \times 10^{12} (1/\text{cm}^2)$ , the momentum relaxation time  $\tau_m = 1 \text{ ps}$  and the effective electron mass  $m^* = 0.042 m_0$  ( $m_0 = 9.1 \times 10^{-31} \text{ kg}$ ) are considered for the 2DEG layer.

The FDTD method is employed to solve (1) - (5) for the proposed HEMT structure. To realize an open boundary a Convolutional Perfectly Match Layer (CPML) is used [17],[18]. In this structure, a thin 2DEG layer is located along  $y$ -axis. The thickness of the 2DEG channel is assumed to be one mesh cell. The mesh size along the channel,  $\Delta y$ , is restricted by the Debye length criteria ( $\Delta y < \sqrt{\epsilon k_B T / (q^2 n_0)}$ ) as well as the 2D plasmon wavelength in the 2DEG layer [10]. Besides, the wavelength of the excitation signal specifies the mesh size along  $x$ -axis,  $\Delta x$ . A non-uniform mesh grid is considered along the  $x$ -axis, to reduce the numerical calculations and the simulation time. In order to decrease the numerical reflections, a smooth transition between the minimum and the maximum mesh sizes along the  $x$ -axis is necessary. Accordingly, a transition length  $\Delta X$ , the increasing cell size rate  $R$ , and the number of cells  $N_{nu}$  must be chosen appropriately by using the relations (8) and (9) [19].

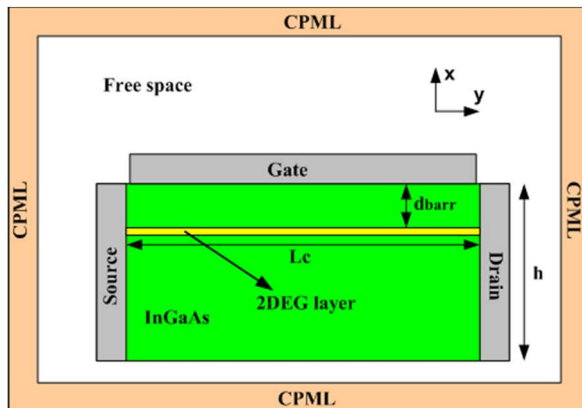


Figure 1. The structure of the proposed gated HEMT.

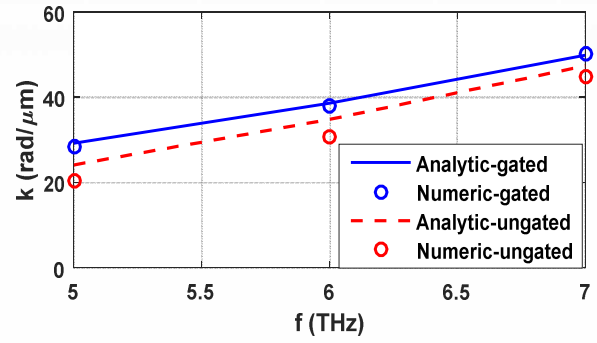


Figure 2. The comparison between the numerical and the analytical dispersion relations of the gated and ungated HEMT.

$$R = (\Delta X + dx_{\text{max}}) / (\Delta X + dx_{\text{min}}), \quad (8)$$

$$N_{nu} = \log(dx_{\text{max}} / dx_{\text{min}}) / \log(R). \quad (9)$$

After choosing the suitable mesh sizes  $\Delta x$  and  $\Delta y$ , the time step  $\Delta t$  is determined based on Courant-Fredrichs-Lewy (CFL) condition for stability using  $\Delta t < 1 / (c \sqrt{(dx_{\text{min}})^{-2} + (dy)^{-2}})$  [20],[21].

The obtained numerical dispersion relations for the 2D plasmon propagation along the 2DEG channel of the unbiased gated and the ungated HEMTs are compared with the analytical values in the frequency range 5-7 THz in Fig. 2. An acceptable agreement between the numerical and analytical results is observed that validates the proposed numerical full wave analysis method. The slight differences between the results are due to the effects of the drain and source PEC contacts and also the limited thickness of the semiconductor that are not considered in the analytical formulations. In the following sections, we have used our proposed full wave model to characterize the HEMT performance.

### III. EFFECTS OF BIAS VOLTAGE ON HEMT CHARACTERISTICS

#### A. Theoretical Consideration

The wave propagation characteristics along the 2DEG channel of plasmonic HEMTs can be controlled by applying appropriate bias voltages. The electron concentration in the channel of a gated HEMT can be approximated by the parallel-plate capacitor relation as follows [22]

$$n_0 = \epsilon \frac{V_g - V_t}{qd_{\text{barr}}}, \quad (10)$$

where  $V_t$  and  $V_g$  are the threshold and the gate voltages, respectively. The threshold voltage can be calculated as [23]

$$V_t = \phi_b - E_c - \frac{qn_d d_{\text{barr}}}{\epsilon}, \quad (11)$$

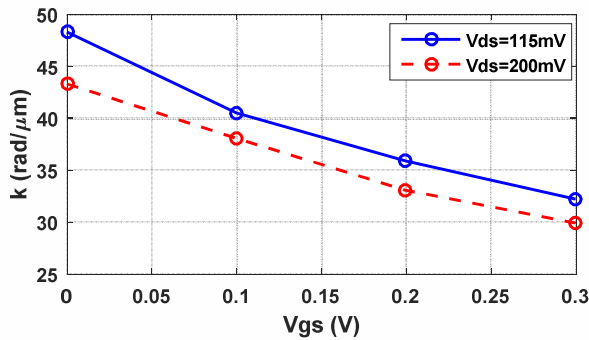
where  $\phi_b$  is the gate Schottky contact barrier height, and is about 0.7eV for metal on III-V compounds. The

conduction band offset value,  $E_c$ , depends on the In mole fraction in InGaAs substrate. Furthermore,  $n_d$  is the delta-doping donor concentration with the value of about  $9.33 \times 10^{11} (1/cm^2)$  at 300K [23].

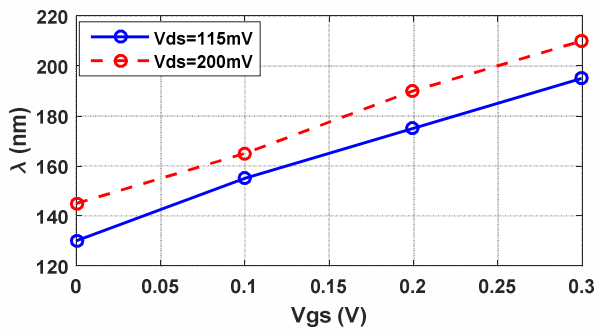
The drain-source  $V_{ds}$  bias voltage controls the average electron velocity in the channel. By employing a voltage  $V_{ds}$  onto the ohmic drain and source terminals, an electric field with the magnitude  $E_0 = V_{ds} / L_c$  is produced along the 2DEG channel. By considering that the device operates in the small signal regime, a linear relation between the electron average velocity and the electric field exists. So, the electrons move with a constant average velocity  $v_0 = E_0 \times q \tau_m / m^*$  [10]. Consequently, it is concluded that the 2D plasmons propagating opposite to this electron velocity confront more attenuations compared to the other ones that causes unsymmetrical propagation of the plasmons along the channel.

**B. Numerical Full Wave Modeling Results**

By considering Fig. 1, the effects of the gate-source and the drain-source bias voltages on the propagation characteristics of the 2D plasmons along the 2DEG layer of the gated HEMT are investigated. All semiconductor parameters are the same with the previous section. The propagation constants and the wavelengths of the 2D plasmons propagating in +y direction are computed at 6THz for different values of the drain-source voltage  $V_{ds}$  and the gate-source voltage  $V_{gs}$ , using the proposed full wave model, and demonstrated in Fig. 3.



(a)



(b)

Figure 3. (a) The phase constants, and (b) the wavelengths of the 2D plasmons propagation in +y direction.

As illustrated in Fig. 3 (a) and (b), by growing both the gate-source  $V_{gs}$  and the drain-source  $V_{ds}$  voltages, the phase constant values are decreased and accordingly the wavelengths of 2D plasmons are increased. Therefore, it is concluded that by varying the bias voltages the propagation properties along the channel HEMTs can be controlled.

Fig. 4 demonstrates the distribution of the electric field close to the channel of the gated HEMT biased at  $V_{gs} = 0.2V$  and  $V_{ds} = 0.2V$ . The excitation signal is proposed to be a single-tone sinusoidal electric field placed at  $y = 2\mu m$  with the frequency 6THz. To excite the plasmons we have introduced a time harmonic electric field of frequency 6THz placed at the middle of the channel, as previously employed in [24] and [11]. In practice, to excite the plasmons in the gated HEMT, first a small gap-discontinuity is created in the gate. Then a plane wave hits the device and the diffracted waves, created due to the gap-discontinuity, are coupled to the 2DEG layer to excite the 2D plasmons [13]. For the ungated HEMT, a small thin metal called the plasmon launcher is used instead of the gap-discontinuity [10]. In fact, the introduced time harmonic electric field, similar to the resultant coupling waves, can create enough momentum to excite the plasmons in our analysis. As illustrated in Fig. 4, the plasmon propagation is confined close to the channel. Also, the 2D plasmon propagates in both  $\pm y$  directions with respect to the excitation point source.

Fig. 5 shows the distribution of the transport variables along the 2DEG channel including: the y-component of the ac electric field, the ac electron velocity, the electron concentration, and the ac electron current density obtained numerically. As shown in the electric field distribution, the effect of wave reflection from the PEC contacts is evident in the drain terminal at  $y = 4\mu m$ . Due to the applied  $V_{ds}$  the 2D plasmons propagate with different phase constants and accordingly different wavelengths in both directions. Moreover, the -y going plasmonic mode is attenuated more quickly compared to the other mode. Thus, applying the bias voltage affects the phase and the decay length of the plasmon propagations along the channel considerably.

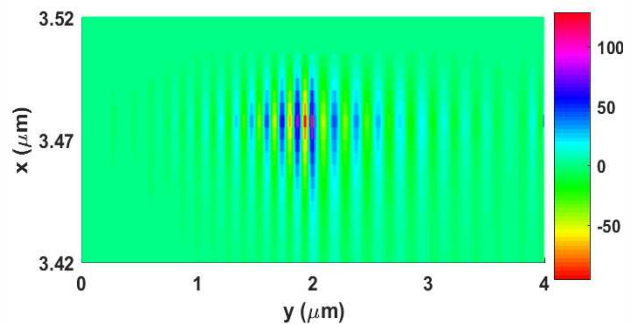


Figure 4. The distribution of the electric field around the channel at 6THz.

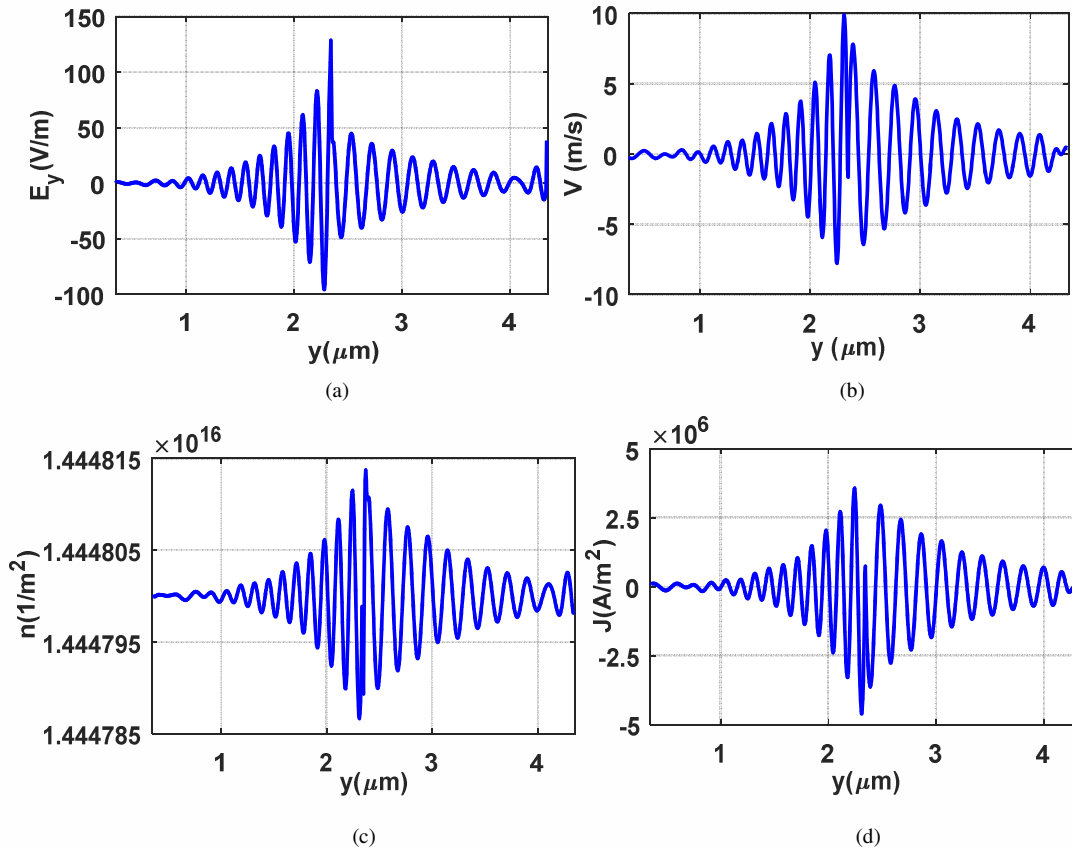


Figure 5. (a) The y-component of the ac electric field, (b) the ac electron velocity, (c) the electron concentration, and (d) the ac current density distributions inside the 2DEG channel at 6THz.

As shown in Fig. 5 (b), (c), and (d), the difference between the phase constants and the attenuation rates of the  $\pm y$  going modes exists in the electron velocity, the electron concentration, and the electron current density distribution curves, too. As a result, our numerical modeling method shows that it is possible to control the 2D plasmon propagation properties by applying the appropriate bias voltages to the PEC contacts.

#### IV. ANALYSIS OF A METALLIC GRATING HEMT

In this section as a practical example, a resonant tunable plasmonic detector based on the biased metallic grating HEMT is analyzed using the proposed full wave model. The resonant detector can be realized at  $\omega \approx \omega_p$  for  $\omega_p \tau_m \gg 1$ , where  $\omega_p$  is plasmon frequency. This kind of detector can be electrically tuned in a wide THz frequency band by varying the gate-source bias voltage and accordingly changing the electron density along the 2DEG layer of the HEMT. The resonant detectors based on the hetero-structures are commonly used for THz spectroscopy [25]-[27].

The proposed grating gate InGaAs HEMT structure is shown in Fig. 6. All parameters are the same with the previous section. The grating is assumed to be made of Au with the electrical conductivity  $\sigma = 5 \times 10^6 (\Omega \cdot m)^{-1}$  [28]. Hence, the effect of the lossy metallic grating is also considered in our numerical analysis. As depicted

in Fig. 6, the periodicity of the grating gate is 200nm with the gate metal length 100nm. To reduce the computations and consequently the simulation time, a non-uniform mesh grid is employed along the x-axis. Therefore, around the channel and the excitation source the cell size is  $\Delta x_{\min} = 5nm$  and far away from them  $\Delta x_{\max} = 100nm$ . Also, the cell size along y-axis is  $\Delta y = 5nm$  that satisfies the Debye length criteria. After determining the mesh sizes, the time step is calculated using the CFL condition.

To excite the plasma wave in grating gate HEMT, an incident wave hits the grating gate and the diffracted waves coupled to the channel to excite the plasmons [10]. By employing a wide band Gaussian excitation pulse as a THz source and extracting the transmission spectra of the device, the detection performance of the structure is studied numerically using the proposed full wave model. The calculated transmission spectra are referenced to the transmission spectra of the device without the grating gate [29]. Also, the tunability of the detection is investigated for different values of the gate bias voltages in THz frequencies.

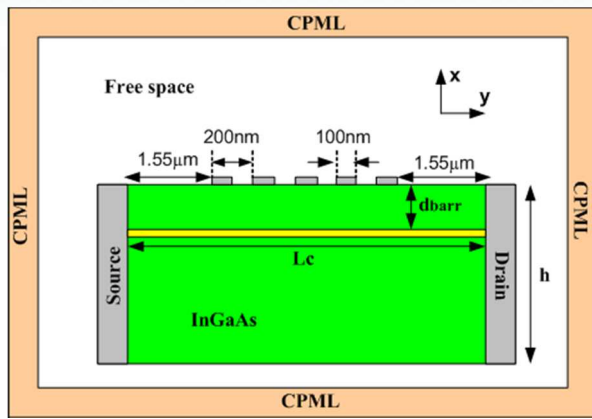


Figure 6. The proposed grating gate HEMT structure.

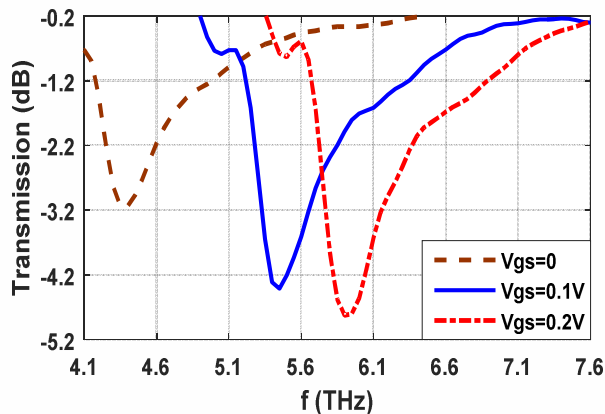


Figure 7. The transmission spectra of the grating gate HEMT structure for different gate bias voltages.

Fig. 7 demonstrates the transmission spectra of the detector for different gate-source bias voltages at  $V_{ds} = 0.115V$  obtained numerically. As shown, by increasing the gate voltage, according to (10), the electron concentration under the gate fingers grows and consequently the plasmon velocity increases that causes a shift in the resonance. Also, the depth of the detection is varied by changing the bias voltages. Therefore, the tunability can be achieved in a broad THz frequency band that is important for plasmonic devices performance. The similar results are reported in [29] by measurement.

## V. CONCLUSION

The analysis and modeling of the 2D plasmon propagation along the 2DEG channel of plasmonic HEMTs were presented, using the full wave hydrodynamic model. To validate the model, the dispersion relations of the gated and ungated HEMTs were calculated both analytically and numerically. Also, the 2D plasmon propagation inside the channel was characterized by employing the various  $V_{ds}$  and  $V_{gs}$ . It was shown that the propagation properties of the plasmons such as the wavelengths and the decay lengths are considerably affected by varying the gate and the drain bias voltages. In this way, the propagation characteristics of the 2D plasmons can be controlled and therefore vast variety of the

reconfigurable plasmonic structures may be realized at THz frequencies. Moreover, as a practical example of these effects, a grating gate HEMT structure was analyzed as a resonant THz detector and its tunability was investigated. It was demonstrated that by changing the gate bias voltage and consequently varying the electron concentration in the channel, the resonant frequency can be tuned in broad THz frequency band. Moreover, this analysis approach makes it possible to obtain the optimum bias voltages and operation point for each application.

## REFERENCES

- [1] V. V. Popov, D. M. Ermolaev, K. V. Maremyanin, N. A. Maleev, and V. E. Zemlyakov, "High-responsivity terahertz detection by on-chip InGaAs/GaAs field-effect-transistor array," *Appl. Phys. Lett.*, vol. 98, pp. 153504-1–153504-3, Apr. 2011.
- [2] A. El Fatimy et al., "Resonant and voltage-tunable terahertz detection in InGaAs/InP nanometer transistors," *Appl. Phys. Lett.*, vol. 89, no. 13, pp. 131926-1–131926-3, Sep. 2006.
- [3] J. K. Choi, V. Mitin, R. Ramaswamy, V. A. Pogrebnyak, M. Pakmehr, A. Muravjov, M. Shur, J. Gill, I. Mehdi, B. S. Karasik, and A. Sergeev, "THz hot-electron micro-bolometer based on low-mobility 2DEG in GaN heterostructure," *IEEE Sensors Journal*, vol. 13, no. 1, pp. 80-88, Jan. 2013.
- [4] B. Sensale-Rodrigues, L. Liu, P. Fay, D. Jena, and H. Grace, "Power amplification at THz via plasma wave excitation in RTD-gated HEMTs," *IEEE Trans. THz Sci. Technol.*, vol. 3, no. 2, Mar. 2013.
- [5] S. Bhardwaj, S. Rajan, and J. L. Volakis, "Analysis of plasmon-modes of a gated bilayer system in high electron mobility transistors," *J. of Appl. Phys.*, May 2016.
- [6] D. Coquillat, S. Nadar, F. Teppe, N. Dyakonova, S. Boubanga-Tombet, W. Knap, et al. "Room temperature detection of sub-terahertz radiation in double-grating-gate transistors," *Opt. Express*, vol. 18, no. 6, pp. 6024-6032, 2010.
- [7] T. Otsuji, T. Watanabe, S. A. B. Tombet, A. Satou, W. M. Knap, V. V. Popov, M. Ryzhii, and V. Ryzhii, "Emission and detection of terahertz radiation using two-dimensional electrons in III-V semiconductors and graphene," *IEEE Trans. THz Sci. Tech.*, vol. 3, no. 1, pp. 63-71, 2013.
- [8] M. A. Khorrami, and S. El-Ghazaly, "Design and analysis of silicon-based terahertz plasmonic switch," *Opt. Express*, vol. 21, no. 21, pp. 25452-25466, 2013.
- [9] M. A. Khorrami, S. El-Ghazaly, S. Q. Yu, and H. Naseem, "THz plasmon amplification using two-dimensional electron-gas layers," *J. of Appl. Phys.*, vol. 111, pp. 09450-1–09450-6, May 2012.
- [10] M. A. Khorrami, S. El-Ghazaly, H. Naseem, and S. Q. Yu, "Global modeling of active terahertz plasmonic devices," *IEEE Trans. on THz Sci. & Technol.*, vol. 4, no. 1, pp. 101- 109, Jan. 2014.
- [11] S. Bhardwaj, N. K. Nahar, S. Rajan, and J. Volakis, "Numerical analysis of terahertz emissions from an ungated HEMT using full-Wave hydrodynamic model," *IEEE Trans. Electron Devices*, vol. 63, no.3, pp. 101- 109, March 2016.
- [12] R. O. Grondin, S. El-Ghazaly, and S. Goodnick, "A review of global modeling of charge transport in semiconductors and full-wave electromagnetics," *IEEE Trans. Microw. Theory Tech.*, vol. 47, no. 6, pp. 817–829, June 1999.
- [13] S. Bhardwaj, B. Sensale-Rodriguez, H. G. Xing, S. Rajan, and J. L. Volakis, "Resonant tunneling assisted propagation and amplification of plasmons in high electron mobility transistors," *J. Appl. Phys.*, vol. 119, no.1, pp. 013102-1–013102-7, 2016.
- [14] M. Hammadi and S. El-Ghazaly, "Air-bridged MESFET: a new structure to reduce wave propagation effect in high

frequency transistors," IEEE Trans. Microw. Theory Tech., vol. 47, pp. 890–899, June 1999.

- [15] S. M. Sohel Imtiaz, and S. M. El-Ghazaly, "Global modeling of millimeter-wave circuits: electromagnetics simulation of amplifiers," IEEE Trans. Microw. Theory Tech., vol. 45, no. 12, pp. 2208-2216, 1997.
- [16] F. J. Crowne, "Contact boundary conditions and the Dyakonov–Shur instability in high electron mobility transistors," J. Appl. Phys., vol. 82, no. 3, p. 1242-1254, Aug. 1997.
- [17] R. Mirzavandeborojeni, A. Abdipour, G. Moradi, and M. Movahhedi, "Unconditionally stable MFLTD method for the full Wave electromagnetic simulation," IEEE Trans. Ant. Prop., vol. 60, no. 5, pp. 2583 - 2586, 01 May 2012.
- [18] A. Taflove and S. C. Hagness, Computational Electrodynamics: The Finite-difference time-domain method, 3rd ed., (Artech House, Norwood, USA, 2005).
- [19] A. Z. Elsherbeni, and V. Demir, The finite-difference time-domain method in electromagnetics with MATLAB® simulations, 2nd edition, (Sci. Tech. Publishing, 2015).
- [20] M. Movahedi, and A. Abdipour, "Efficient numerical methods for simulation of high-frequency active devices," IEEE Trans. Microw. Theo. & Tech., vol. , no. 6, pp. 2636-2645, June 2006.
- [21] Y.A. Hussein, S.M. El-Ghazaly, and S.M. Goodnick, "An efficient electromagnetic-physics-based numerical technique for modeling and optimization of high-frequency multifinger transistors", IEEE Trans. Microw. Theory Tech., vol. 51, no. 12, pp. 2334 - 2346, Dec. 2003.
- [22] M. Dyakonov, and M. Shur, "Shallow water analogy for a ballistic field effect transistor: new mechanism of plasma wave generation by dc current," Phys. Rev. Lett., vol. 71, pp. 2465–2468, Oct. 1993.
- [23] H. Saxena, R. E. Peale, and W. R. Buchwald, "Tunable two-dimensional plasmon resonances in an InGaAs/InP high electron mobility transistor," J. Appl. Phys., vol. 105, pp. 113101–113106, June 2009.
- [24] A. Eguliz, T. K. Lee, J. J. Quinn, and K. W. Chiu, "Interface excitations in metal-insulator-semiconductor structures," Phys. Rev. B, vol. 11, pp. 4989–4993, Jun. 1975.
- [25] F. Daneshmandian, A. Abdipour, and A. N. Askarpour, "Full wave analysis of terahertz dispersive and lossy plasmonic HEMT using hydrodynamic model", J. Opt. Soc. Am. B, vol. 36, no. 4, pp. 1138-1143, 2019.
- [26] J.-Q. L'u, M. S. Shur, J. L. Hesler, L. Sun, and R. Weikle, "Terahertz detector utilizing two-dimensional electronic fluid," IEEE Electron Device Lett. , vol. 19, no. 10, pp. 373-375, Oct. 1998.
- [27] T. Watanabe, S. A. Boubanga-Tombet, Y. Tanimoto, D. Fateev, and V. Popov, "InP- and GaAs-Based plasmonic high-electron-mobility transistors for room-temperature ultrahigh-sensitive terahertz sensing and imaging," IEEE Sensors J., vol. 13, no. 1, pp. 89-99, Jan. 2013.
- [28] M. Hövel, B. Gompf, and M. Dressel, "Dielectric properties of ultrathin metal films around the percolation threshold," Phys. Rev. B, vol. 81, no. 3, pp. 035402-1–035402-8, 2010.
- [29] A. V. Muravjov, D. B. Veksler, V. V. Popov, O. V. Polischuk, and N. Pala, "Temperature dependence of plasmonic terahertz absorption in grating-gate gallium-nitride transistor structures," Appl. Phys. Lett., vol. 96, no. 4, pp. 042105-1–042105-3, 2010.



**Farzaneh Daneshmandian** received the B.S. and M.S.C. degrees in electrical engineering from Amirkabir University of Technology (Tehran polytechnic), Tehran, Iran, in 2011 and 2013, respectively. Her research areas include Modeling and Analysis of Millimeter-Wave/THz Active Plamonic devices, Numerical Modeling of Plamonic devices, Nonlinear Design and Analysis of RF/Microwave Circuit.

She is currently pursuing the Ph.D. degree with the Amirkabir University of Technology, Tehran, Iran.



**Abdolali Abdipour** was born in Alashtar, Iran, in 1966. He received his B.Sc. degree in Electrical Engineering from Tehran University, Tehran, Iran, in 1989, his M.Sc. degree in electronics from Limoges University, Limoges, France, in 1992, and his Ph.D. degree in electronic engineering from Paris XI University, Paris, France, in 1996. He is currently a professor

with the Electrical Engineering Department, Amirkabir University of Technology (Tehran Polytechnic), Tehran, Iran. He has authored five books. His research areas include Wireless Communication Systems (Rf Technology and Transceivers), Rf/Microwave/ Millimeter-Wave/Thz Circuit and System Design, Electromagnetic (Em) Modeling of Active Devices and Circuits, High-Frequency Electronics (Signal and Noise), Nonlinear Modeling, and Analysis of Microwave Devices and Circuits. He has authored or coauthored over 330 papers in refereed journals and local and international conferences.



**Amir Nader Askarpour** received the B.S. degree in Electrical Engineering from the Sharif University of Technology, Tehran, Iran, in 2004 and the M.S.C. and Ph.D. degrees from the University of Tehran, Tehran, Iran, in 2006 and 2012, respectively. From 2012 to 2014, he was a Postdoctoral Research Associate at University of Texas at Austin, TX, USA.

He is currently an Assistant Professor with the Amirkabir University of Technology, Tehran, Iran.